INT. J. NUM. METH. HEAT FLUID FLOW, VOL. 4, 329–345 (1994)

A COMPLEMENTARY VOLUME APPROACH FOR MODELLING THREE-DIMENSIONAL NAVIER–STOKES EQUATIONS USING DUAL DELAUNAY/VORONOI TESSELLATIONS

J. C. CAVENDISH

Mathematics Department, General Motors Research Laboratories, Warren, MI 48090, USA

C. A. HALL* AND T. A. PORSCHING*

Department of Mathematics and Statistics, University of Pittsburgh, Pittsburgh, PA, USA

ABSTRACT

We describe a new mathematical approach for deriving and solving covolume models of the three-dimensional, incompressible Navier–Stokes flow equations. The approach integrates three technical components into a single modelling algorothm: automatic grid generation; covolume equation generation; dual variable reduction.

KEY WORDS Navier–Stokes equations Delaunay/Voronoi tessellations

INTRODUCTION

In recent years covolume methods based on a dual pair of mutually orthogonal companion grids have gained the attention of the CFD community and have been used for the numerical modelling of fluid flows[5,6,13–15,17–19,23,26]. The basic idea behind the derivation of these schemes is to exploit the divergence/curl form of the underlying conservative laws by integrating them over the covolumes and, using the divergence theorem and Stokes' theorem, converting volume integrals into surface and line integrals on the boundaries of the volumes, whereupon these integrals are then discretized.

In this paper we extend from two to three-dimensions a covolume approach proposed[5,6,12–14] for modelling the flow of a viscous incompressible fluid in an open bounded domain. The approach combines three components:

(1) *Unstructured grid generation:* an algorithm presented at MAFELAP[3,4] is used to discretize the flow domain into a tetrahedral Delaunay tessellation and companion Voronoi polyhedral decomposition.
(2) *Covolume equation generation:* the continuity equation is discretized by integrating it over each tetrahedron. The divergence theorem and Stokes' theorem are used to derive finite volume analogues of a scalar form of the momentum equations in terms of the primitive variables of normal velocity components and pressure (assigned to the edges and corners, respectively, of Voronoi polyhedra).

*This research partially supported by the Electric Power Research Institute Grant No. RP:8006-24.

0961–5539/94/040329–18$2.00

Received November 1993

(3) *Dual variable reduction:* a network theoretical technique is used to transform the covolume system of equations into an equivalent system (called the dual variable system) which is a factor of *three* smaller than the original primitive covolume system.

The paper is organized as follows. First, we briefly review our approach (the so-called Watson algorithm[25] for constructing tessellations of mutually orthogonal Delaunay tetrahedra and Voronoi polytopes. We then present the particular form of the 3D incompressible Navier–Stokes equations that will be used in the following section to generate continuous time, discrete space covolume difference equations for the continuum flow problem. We next present a method for the reconstruction of a velocity vector field from the (*scalar*) velocity components determined by the covolume method.

We then outline an approach whereby the covolume system of equations involving primitive flow variables is transformed into an equivalent system which is one-third the size of the original primitive system. In the next section we establish an equivalence between the covolume method and the MAC scheme for hexahedral uniform meshes for the simple case of Stokes flow. Conclusions are given in the final section.

UNSTRUCTURED GRID GENERATION

At MAFELAP V (1984) an algorithm was described for the computer generation of Delaunay tetrahedral finite element meshes for bounded three-dimensional domains[3,4]. The approach to solid mesh generation, called Watson's algorithm[25], turns upon the simple observation that four points in space will determine a Delaunay tetrahedron if and only if the circumsphere passing through these points contains no other points in its interior. In effect, Watson's approach is to reject (from the set of all possible tetrahedra that might be formed in a tessellation of a given set of points) those tetrahedra with non-empty associated circumspheres.

Closely associated with the Delaunay mesh of tetrahedra is a dual construct called the Voronoi tessellation. Each point, p, in the tetrahedral mesh is surrounded by a union of disjoint tetrahedra, say T_p. Appropriate straight-line connections of the circumcentres of these tetrahedra[3,4,8] produces the edges of a convex polytope, V_p, containing p in its interior. The Voronoi polytope, V_p, has the property that any point in its interior is closer to p than it is to any other point in the mesh. Consequently, the faces of V_p are composed of bounded planes that bisect tetrahedral edges connecting p to its neighbouring points in the mesh. On the other hand, an edge on the surface of V_p is perpendicular to a triangle face contained in T_p and that edge passes through the circumcentre of that triangle face. As a result of all this, V_p and T_p share a mutual orthogonality which we summarize as follows:

(1) faces of V_p are perpendicular bisectors of edges of tetrahedra in T_p;
(2) edges of V_p are perpendicular to triangle faces in T_p and pass through tetrahedral and (triangle) facial circumcentres in T_p;
(3) Corners on the surface of V_p are circumcentres of tetrahedra in T_p.

Visualization and manipulation of three-dimensional tetrahedral meshes and Voronoi polytopes is difficult at best (it is undoubtedly one of the principal reasons many users avoid the tetrahedral element in mesh construction). To help with this, and to lay the foundation for covolume equation generation later, we consider some simple illustrations. These illustrations consider a single point p_1, a single set of surrounding tetrahedra, T_{p_1}, and a simple associated Voronoi polytope, V_{p_1}, all extracted from a Delaunay tetrahedral mesh of a large set of points containing p_1. *Figure 1a* displays the triangular faceted surface of T_{p_1} containing 30 tetrahedra, each possessing p_1 as a vertex. Looking inside T_{p_1}, we extract the Voronoi polytope V_{p_1} shown in *Figure 1b*. Note that in general, the corners on ∂V_{p_1} are shared by three faces on ∂V_{p_1}. This means that such a vertex is also a vertex on three abutting Voronoi polytopes, V_{p_2}, V_{p_3}, V_{p_4}.

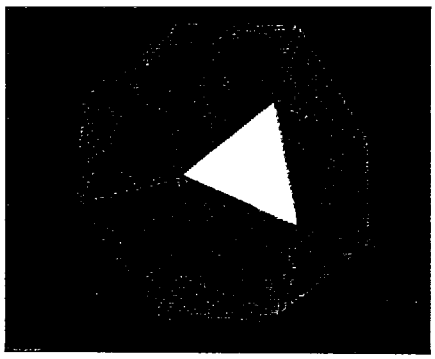

Figure 1a Surface of T_{p_1}

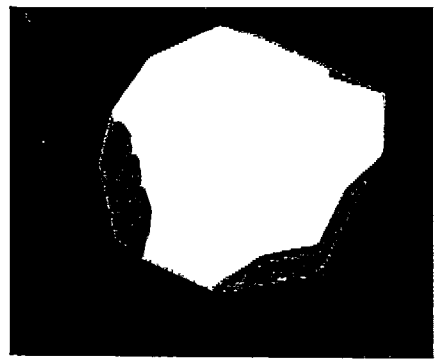

Figure 1b Voronoi polytope associated with p_1

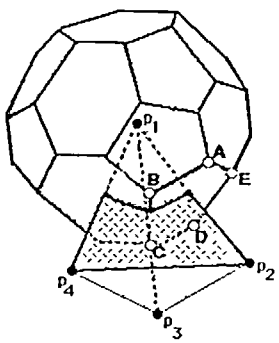

Figure 1c Polytope and one tetrahedron

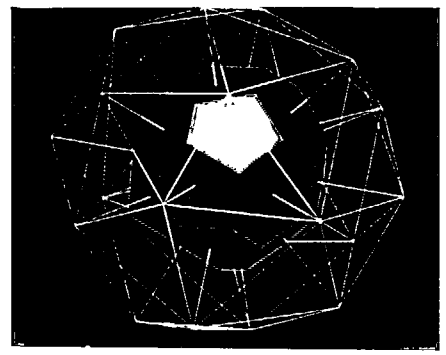

Figure 1d T_{p_1} and Voronoi polyhedron V_{p_1}

Connecting p_1, p_2, p_3, p_4 forms one of the Delaunay tetrahedra in T_{p_1} (see *Figure 1c*). *Figure 1d* illustrates T_{p_1} (wire frame mode) and V_{p_1} (shaded mode) simultaneously. From *Figures 1c* and *1d*, the mutual orthogonality of T_{p_1} and V_{p_1} is evident. For example, edge $\overline{p_1p_2}$ is perpendicular to and is bisected by face ABCDE of the polytope V_{p_1}. Also, edge $\overline{BC}$ of V_{p_1} is perpendicular to and passes through the circumcentre of face $\overline{p_1p_2p_4}$.

We conclude with several comments that will be important in what follows. First, the covolume discretizations described later make it desirable that a Delaunay tetrahedron contain its circumcentre and that the circumcentre of anyone of its four triangular faces lie within that face. Although this situation cannot be guaranteed for a Delaunay tessellation of a random set of points, it is closely approximated when the variation of point spacing is reasonably smooth throughout the domain.

Second, degeneracies can occur in 3D Delaunay tessellations in one of two ways. When more than 4 points lie on a sphere, the Watson algorithm has to be adjusted so that correct and consistent decisions are made regarding formation of Delaunay tetrahedra. This can be accomplished by perturbing the coordinates of points when ambiguity occurs[3,4]. This in turn can produce Voronoi polyhedra which have faces of zero area or edges that have zero length. This situation apparently does not adversely affect the covolume discretizations as will be shown later.

Perturbing points can also produce what are termed *slivers*[3,4]: collapsed tetrahedra with arbitrarily small (and in extreme cases even zero) volume, but well proportioned triangular faces. Such a tetrahedral element would spell computational trouble if used in finite element analysis. For the covolume method presented here, this type of degeneracy presents no apparent problem, as we show later.

A pair of Delaunay and Voronoi tessellations of Ω is called *ideal* if:

(i) there are no tetrahedra of zero volume,
(ii) every face of a Voronoi polytope has positive area and each edge of the face has positive length,
(iii) every tetrahedral circumcentre is contained within the interior of the associated tetrahedron, and
(iv) every circumcentre of a tetrahedral face is contained within the interior of the associated triangular face.

Unfortunately, it is virtually impossible to guarantee an ideal pair of tessellations with contemporary solid mesh generation technology. In fact, it is worth noting that even in two dimensions, we know of no automatic mesh generator that guarantees acute triangulations, a necessary condition that circumcentres are contained in associated triangles. Thus any serious effort to implement a covolume method in three dimensions must confront and resolve the problems that arise when the tessellation fails to be ideal. One of our objectives in this paper is to address these issues.

In *Figure 2* we show a Delaunay tetrahedral mesh of a flow duct containing 1000 tetrahedra. *Figure 3* illustrates a rendering of the dual Voronoi tessellation containing 500 polytopes (polytopes interior to the flow region only).

THE INCOMPRESSIBLE FLOW PROBLEM

We consider a bounded flow domain Ω in R^3 with boundary $\partial\Omega$. The continuum problem[20] is to find a velocity $\mathbf{q} = (u(x, y, z, t), v(x, y, z, t), w(x, y, z, t))^T$ and a scalar pressure field $p(x, y, z, t)$ which satisfy the continuity, or *conservation of mass*, equation:

$$\nabla \cdot \mathbf{q} = 0, \qquad (x, y, z) \in \Omega,\ t > 0 \tag{1}$$

and the vector-valued *conservation of momentum* equation

$$\frac{\partial \mathbf{q}}{\partial t} - \nu \nabla^2 \mathbf{q} + (\mathbf{q} \cdot \nabla)\mathbf{q} + \nabla p = \mathbf{F}(\mathbf{x}, t) \tag{2}$$

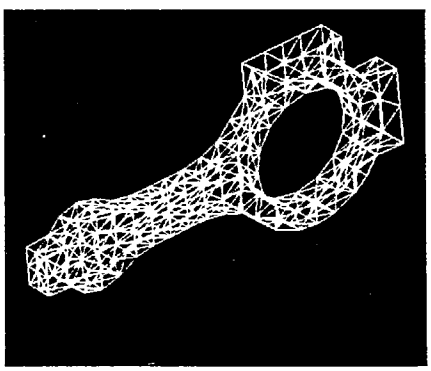

Figure 2 Delaunay tessellation in 3D

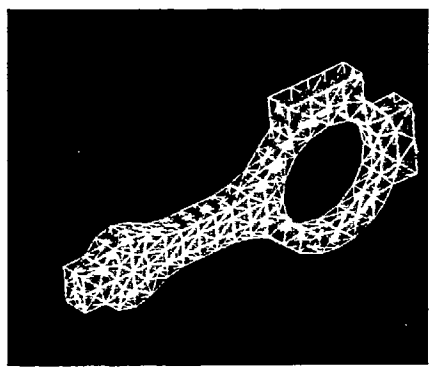

Figure 3 Voronoi tessellation in 3D

where $\mathbf{x} = (x, y, z)$, v is the kinematic viscosity of the fluid and $\mathbf{F}(\mathbf{x}, t)$ is a prescribed source term. We assume boundary conditions of the form:

$$p(\mathbf{x}, t) = p_b(\mathbf{x}), \qquad \mathbf{x} \in \partial\Omega_1,\ t > 0 \tag{3}$$

and

$$\mathbf{q}(\mathbf{x}, t) = \mathbf{q}_b(\mathbf{x}), \qquad \mathbf{q} \in \partial\Omega_2,\ t > 0 \tag{4}$$

where $\partial\Omega = \partial\Omega_1 \cup \partial\Omega_2$ and $\partial\Omega_1 \cap \partial\Omega_2 = \phi$. Further, we assume initial conditions of the form:

$$\mathbf{q}(\mathbf{x}, 0) = \mathbf{q}_0(\mathbf{x}), \qquad p(\mathbf{x}, 0) = p_0(\mathbf{x}),\ \mathbf{x} \in \Omega \tag{5}$$

Following earlier development[13–15], we make use of (1) to first represent the convective and viscous terms in (2) as, respectively,

$$(\mathbf{q}\cdot\nabla)\mathbf{q} = \nabla\cdot(\mathbf{q}\mathbf{q}^{\mathrm{T}}) \tag{6}$$

and

$$\nabla^2\mathbf{q} = -\mathbf{curl}(\mathbf{curl}\ \mathbf{q}) \tag{7}$$

For a constant unit vector $\mathbf{n}$ it can be verified that:

$$[\nabla\cdot(\mathbf{q}\mathbf{q}^{\mathrm{T}})]\cdot\mathbf{n} = [\nabla(\mathbf{q}\cdot\mathbf{n})]\cdot\mathbf{q} = \|\mathbf{q}\|\left[\frac{\partial}{\partial\mathbf{q}}(\mathbf{q}\cdot\mathbf{n})\right] \tag{8}$$

where $\partial/\partial\mathbf{q}$ denotes the directional derivative in the direction $\mathbf{q}$ and $\|\mathbf{q}\|$ is its Euclidean length. Substituting (6) and (7) into (2) and taking the inner product with the unit vector $\mathbf{n}$ (and using (8)), we obtain a *scalar* version of the momentum equation:

$$\frac{\partial}{\partial t}(\mathbf{n}\cdot\mathbf{q}) + v\,\mathbf{curl}(\mathbf{curl}\ \mathbf{q})\cdot\mathbf{n} + \|\mathbf{q}\|\frac{\partial}{\partial\mathbf{q}}(\mathbf{q}\cdot\mathbf{n}) + \frac{\partial p}{\partial\mathbf{n}} = \mathbf{n}\cdot\mathbf{F} \tag{9}$$

It is (1) and (9) to which we apply the covolume technique in the following section.

COVOLUME DISCRETIZATION OF THE FLOW PROBLEM

In the two-dimensional covolume method the continuity equation is integrated over each triangle in a mesh of triangles, the divergence theorem is applied, and the normal velocity component $\mathbf{n}\cdot\mathbf{q}$ is approximated by mid-edge normal velocity components[13–15,17–19]. In the three-dimensional setting, we integrate (1) over each tetrahedral control volume, $\hat{\Omega}_j$ (see *Figure 5*), apply the divergence theorem and approximate the normal velocity component $\mathbf{n}\cdot\mathbf{q}$ by velocity components normal to the faces of the tetrahedra and passing through facial circumcentres. (Recall that the edges of Voronoi polytopes are normal to the tetrahedral faces and pass through the circumcentres of these faces.) The result is:

$$0 = \int\int\int_{\hat{\Omega}_j} \nabla\cdot\mathbf{q}\,\mathrm{d}V = \int\int_{\partial\hat{\Omega}_j} \mathbf{q}\cdot\mathbf{n}\,\mathrm{d}\sigma \simeq \sum_{i=1}^{4} u_i(t)A_i(\mathbf{n}\cdot\mathbf{n}_i) \tag{10}$$

where $\mathbf{n}$ is the outward normal vector to $\partial\hat{\Omega}_j$, $\mathbf{n}_j$ is a pre-assigned unit normal to the ith face of $\partial\hat{\Omega}_j$, A_i is the area of the ith face of $\hat{\Omega}_j$, $u_i(t) = \mathbf{q}\cdot\mathbf{n}_i|_{P_i}$ and P_i is the circumcentre of the ith face of $\hat{\Omega}_j$. Note that $(\mathbf{n}\cdot\mathbf{n}_i) = \pm 1$. As pointed out earlier, this circumcentre P_i, may be outside of the ith face of $\hat{\Omega}_j$. When this occurs, we also assume that $u_i(t)$ is an approximation to the flow normal to the ith face. If there are N_T tetrahedra in the tessellation of Ω, then there are N_T such discrete continuity equations which we write as:

$$\mathbf{A}\mathbf{D}_1\mathbf{u}(t) = \mathbf{b} \tag{11}$$

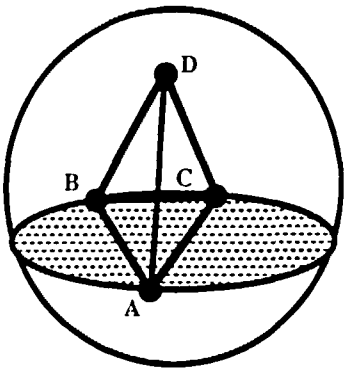

Figure 4a Delaunay tetrahedron and associated circumsphere

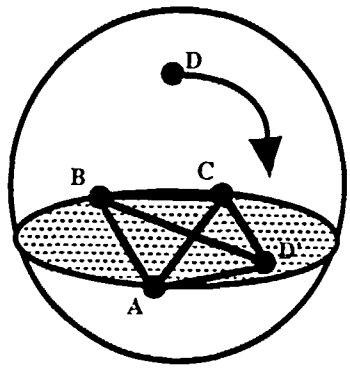

Figure 4b Distorted Delaunay tetrahedron

where $\mathbf{u}(t)$ is an N_F-vector of normal velocity components with ith entry $u_i(t)$, and N_F is the number of triangular faces in the tetrahedral mesh for which the normal velocity is unknown. The diagonal matrix $\mathbf{D}_1$ has its ith entry equal to A_i. The vector $\mathbf{b}$ contains known boundary data (that is, velocities specified in (4)). The $N_T \times N_F$ matrix $\mathbf{AD}_1$ is called the *discrete divergence operator* associated with the tetrahedral Delaunay tessalation. We note also that the entries of the matrix A are ± 1 or 0. This fact will be used later.

A problem which arises in three-dimensional mesh generation is the possible creation of *slivers*[3,4]. In *Figure 4a* we illustrate a Delaunay tetrahedron together with its associated circumsphere. If the node point **D** in *Figure 4a* is moved to any other position on the circumsphere, then the tetrahedron **ABCD** remains a valid Delaunay tetrahedron. As a worst case, suppose **D** were moved to point **D'** shown in *Figure 4b*, where **D'** is slightly out of the plane defined by nodes **A**, **B** and **C**. **ABCD'** then defines a badly distorted Delaunay tetrahedron whose faces are well-proportioned triangles, but whose volume can be made arbitrarily small. We refer to these thin tetrahedra as *slivers*. Although hard to avoid, most slivers can be removed by techniques described in References 3, 4. We impose the discrete continuity equation (10) for all tetrahedra; even in the extreme case when the volume of $\hat{\Omega}_j$ is zero. This is reasonable even for the latter case since (10) then simply states that the flow is continuous across the planar region composed of the faces of $\hat{\Omega}_j$.

The momentum equation (in scalar form defined by (9)) is approximated at the circumcentre of each face of the N_F faces of the tetrahedral mesh bearing an unknown normal velocity component as follows: with reference to *Figure 5* and starting with facial circumcentre node P_1 in *Figure 5*, we take $\mathbf{n} = \mathbf{n}_1$ in (9) where $\mathbf{n}_1$ is the unit vector through P_1 normal to the triangular face denoted **ABC**. Then, we define the following discretizations:

I. Temporal term: $\dfrac{\partial}{\partial t}(\mathbf{n}\cdot\mathbf{q})$

$$\frac{\partial}{\partial t}(\mathbf{n}_1\cdot\mathbf{q})|_{P_1} = \frac{\mathrm{d}}{\mathrm{d}t}u_1(t) \tag{12}$$

II. Pressure term: $\dfrac{\partial p}{\partial \mathbf{n}}$

$$\frac{\partial p}{\partial \mathbf{n}_1} \simeq \frac{p_2(t) - p_1(t)}{\|Q_2 - Q_1\|} \tag{13}$$

where p_1 approximates pressure at the circumcentre, Q_1 of tetrahedron **ABCD** and p_2 approximates pressure at circumcentre Q_2 of tetrahedron **ABCE** (see *Figure 5*).

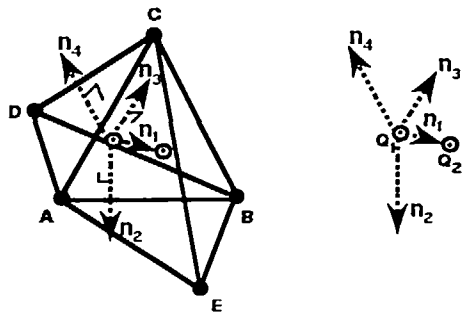

Figure 5 Tetrahedral control volume $\hat{\Omega}_j$ with the vertices A, B, C, D

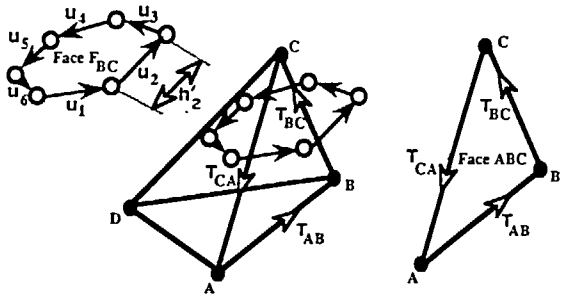

Figure 6 Tetrahedral face ABC and Voronoi face $\mathbf{F_{BC}}$

III. Viscous term: **curl(curl q)·n**

If $A_{\mathbf{ABC}}$ is the area of triangular face **ABC**, then

$$\mathbf{curl(curl\ q)}\cdot\mathbf{n}_1 \simeq \frac{1}{A_{\mathbf{ABC}}} \int\int_{\mathbf{ABC}} (\mathbf{curl\ curl\ q})\cdot\mathbf{n}_1\, d\sigma \tag{14}$$

Let **T** be a unit tangent vector to ∂(**ABC**) oriented in the counterclockwise direction with respect to $\mathbf{n}_1$.

Then, by Stokes' theorem:

$$\int\int_{\mathbf{ABC}} (\mathbf{curl\ curl\ q})\cdot\mathbf{n}_1\, d\sigma = \int_{\partial(\mathbf{ABC})} \mathbf{curl\ q}\cdot\mathbf{T}\, ds$$

$$= \int_{\mathbf{AB}} \mathbf{curl\ q}\cdot\mathbf{T}_{\mathbf{AB}}\, ds + \int_{\mathbf{BC}} \mathbf{curl\ q}\cdot\mathbf{T}_{\mathbf{BC}}\, ds + \int_{\mathbf{CA}} \mathbf{curl\ q}\cdot\mathbf{T}_{\mathbf{CA}}\, ds \tag{15}$$

where $\mathbf{T_{AB}}$, $\mathbf{T_{BC}}$ and $\mathbf{T_{CA}}$ are the three unit tangent vectors to the sides of triangle face **ABC** (see *Figure 6*). Because of the mutual orthogonality of Delaunay tetrahedral and Voronoi polyhedral tessellations, these tangent vectors are normal vectors to the faces (hyperplanes bisecting edges **AB**, **BC** and **CA**) of three abutting Voronoi polyhedra. Also,

$$\int_{\mathbf{BC}} \mathbf{curl\ q}\cdot\mathbf{T}_{\mathbf{BC}}\, ds \simeq h_{\mathbf{BC}}(\mathbf{curl\ q})_{(\mathbf{B}+\mathbf{C})/2}\cdot\mathbf{T}_{\mathbf{BC}} \tag{16}$$

where $h_{\mathbf{BC}}$ is the length of edge **BC**.

Next, if F_{BC} is the Voronoi polyhedral face corresponding to the plane bisecting **BC**, then*:

$$(\mathbf{curl}\ \mathbf{q})_{(B+C)/2} \cdot \mathbf{T}_{BC} \simeq \frac{1}{\text{area}(F_{BC})} \int\int_{F_{BC}} \mathbf{curl}\ \mathbf{q} \cdot \mathbf{T}_{BC}\, d\sigma \tag{17}$$

Because $\mathbf{T}_{BC}$ is normal to F_{BC}, a second application of Stokes' theorem to (17) yields:

$$\int\int_{F_{BC}} \mathbf{curl}\ \mathbf{q} \cdot \mathbf{T}_{BC}\, d\sigma = \int_{\partial F_{BC}} \mathbf{q} \cdot \mathbf{n}\, ds \tag{18}$$

where $\mathbf{q} \cdot \mathbf{n}$ is the component of flow tangential to the edges of F_{BC}, and therefore, normal to certain triangle faces of the tetrahedral mesh. Finally, we have:

$$\int_{\partial F_{BC}} \mathbf{q} \cdot \mathbf{n}\, ds \simeq \sum_{i=1}^{k} u_i(t) h_i' (\mathbf{n} \cdot \mathbf{n}_i) \tag{19}$$

where h_i' are the lengths of the k ($= 6$ in *Figure 6*) edges bounding the polyhedral face F_{BC}. Note that in the pressure discretization (13), $\|Q_2 - Q_1\|$ is also the length of an edge of a Voronoi polyhedron. If an edge of a Voronoi polytope has zero length (some $h_i' = 0$), then this edge contributes nothing to the boundary integral in (19) and our approximation in (19) is consistent since the corresponding summand is zero. With reference to (13), for such an edge, $Q_2 = Q_1$, and $\partial p_1 / \partial \mathbf{n}_1$ is set to zero; the pressures $p_2(t)$ and $p_1(t)$ are equal since $Q_2 = Q_1$. Implementation would not, however, require special treatment since the discrete momentum equation is ultimately scaled by $\|Q_2 - Q_1\|$ (see (27)). Combining (18) and (19) with (16) produces:

$$\int_{BC} \mathbf{curl}\ \mathbf{q} \cdot \mathbf{T}_{BC}\, ds \simeq \frac{h_{BC}}{\text{area}(F_{BC})} \sum_{i=1}^{k} u_i(t) h_i' (\mathbf{n} \cdot \mathbf{n}_i) \tag{20}$$

Similarly, $\int_{CA} \mathbf{curl}\ \mathbf{q} \cdot \mathbf{T}_{CA}\, ds$ and $\int_{AB} \mathbf{curl}\ \mathbf{q} \cdot \mathbf{T}_{AB}\, ds$ can be approximated by linear combinations of normal velocity components, $u_i(t)$, assigned to the edges of polyhedral faces that are hyperplanes bisecting **CA** and **AB** respectively. Finally, (14) indicates that $\mathbf{curl}(\mathbf{curl}\ \mathbf{q}) \cdot \mathbf{n}_1$ can be approximated by a sum of tangential flows along polyhedral edges (hence, components of flow, $u_i(t)$, normal to triangle faces of tetrahedral covolumes) corresponding to hyperplanes bisecting **AB**, **BC**, and **CA**.

IV. Convective term: $\|\mathbf{q}\| \dfrac{\partial}{\partial \mathbf{q}} (\mathbf{q} \cdot \mathbf{n})$

We construct an upwind approximation to the convective term by extending the approach, in Reference 15, to three dimensions. This is a two step process.

Step 1: Determine an approximation to the velocity at the vertices of each tetrahedron. Let p_i be a vertex of tetrahedron $\bar{\Omega}_j$ and V_{p_i} be the Voronoi polytope associated with p_i. Further, let T_{p_i} be the set of all tetrahedra that share vertex p_i and S_{p_i} be the set of circumcentres of those faces of the tetrahedra in the set T_{p_i} that have p_i as a vertex. The point p_i is in the convex hull of S_{p_i}. Note that the facial circumcentre P_k may be outside of the kth face; however, the velocity $u_k(t)$ is associated with P_k.

The velocity vector $\mathbf{q}$ at vertex p_i can be approximated (in several ways) as a linear combination of the velocities at the facial circumcentres in S_{p_i}; assuming the latter are known (see next section). For example, choose four points P_k in S_{p_i}, $k = 1, 2, 3, 4$, such that the tetrahedron with vertices $\{P_k\}_{k=1}^{4}$ contains p_i (see *Figure 7*). Note that tetrahedron $\overline{P_1P_2P_3P_4}$ is not a tetrahedron

*As pointed out earlier, we cannot guarantee the area of face F_{BC} is positive. In fact, face F_{BC} could degenerate to a line or even a point. For such cases the approximation in (17) is invalid. See later for an example of how the need for this approximation can be circumvented.

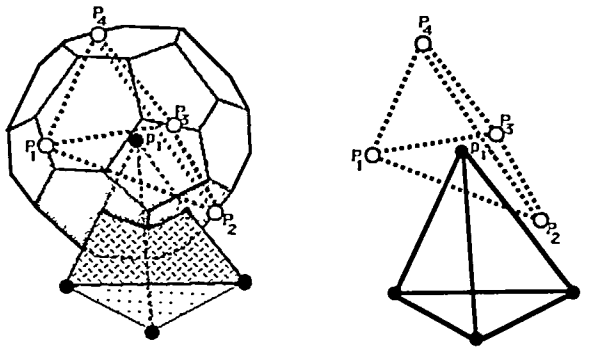

Figure 7 Voronoi polytope V_{p_1} associated with vertex p_i and an enclosing tetrahedron

of the original Delaunay tessellation. The velocity $\mathbf{q}(p_i)$ is approximated by:

$$\mathbf{q}(p_i) \doteq \sum_{k=1}^{4} \beta_{ik}\mathbf{q}(P_k) \tag{21}$$

where $\{\beta_{ik}\}_{k=1}^{4}$ are the barycentric coordinates of the point p_i in the tetrahedron $\overline{P_1P_2P_3P_4}$. Note that the choice of the P_k and the determination of the coordinates β_{ik} need only be done once in a preprocessor stage.

Step 2: Upwind differencing of convection term. Let P_1 be a facial circumcentre where the convection term is to be discretized and $\mathbf{q}(P_1)$ be the velocity vector at P_1 (from the previous time step). Assume $\mathbf{n}_1$ is an outward normal to the triangular face **ABC** with circumcentre P_1. The upwind strategy then involves testing whether $\mathbf{q}(P_1)\cdot\mathbf{n}_1 \geqslant 0$; i.e. the flow across the face is out of tetrahedron $\hat{\Omega}_j$ in *Figure 8*. (If $\mathbf{q}(P_1)\cdot\mathbf{n}_1 < 0$ then consider the other abutting tetrahedron sharing face **ABC**.)

Let Q be the point of intersection of the vector $-\mathbf{q}(P_1)$ with a face (say **ABD**) of $\hat{\Omega}_j$. Then:

$$\|\mathbf{q}\| \frac{\partial}{\partial \mathbf{q}}(\mathbf{q}\cdot\mathbf{n}_1) \doteq \|\mathbf{q}(P_1)\| \frac{(\mathbf{q}(P_1)\cdot\mathbf{n}_1 - \mathbf{q}(Q)\cdot\mathbf{n}_1)}{\|P_1Q\|} \tag{22}$$

The velocity $\mathbf{q}(Q)$ is determined by linear interpolation of the velocity at the vertices **A**, **B**, **D**, the latter having been determined in Step 1.

If the facial circumcentre P_1 is not on the face $\overline{\mathbf{ABC}}$, then replace P_1 in the above discussion by the *centroid* of that face. In such a case, as earlier, we assume $\mathbf{q}(P_1)\cdot\mathbf{n}_1$ is a good approximation to the flow across face **ABC** in the direction $\mathbf{n}_1$.

Combining (12)–(15), (20) and (22), we obtain a semi-discrete momentum equation of the form:

$$\frac{d\mathbf{u}}{dt} + Q(\mathbf{u})\mathbf{u} = D_2^{-1}A^{\mathrm{T}}\mathbf{p} + \mathbf{b} \tag{23}$$

where $Q(\mathbf{u})$ is an $N_F \times N_F$ matrix containing couplings associated with the discretization of the viscous and convective terms, the latter depending on $\mathbf{u}$. The $N_F \times N_F$ diagonal matrix D_2 has as its ith entry, the distance between the two circumcentres of the two tetrahedra sharing the ith triangular face in the mesh; see (13). The vector $\mathbf{p}$ of pressures is $N_T \times 1$ and the matrix A^{T} is the transpose of the $N_T \times N_F$ matrix in (11); a fact that we exploit in a later section.

Equations (11) and (23) form a differential algebraic equation (DAE) system of $(N_T + N_F)$ equations in $(N_T + N_F)$ unknowns; the N_T pressures and the N_F velocity components. This system could be solved using any one of a variety of DAE solvers to obtain a numerical solution of the fluid dynamics system (1) and (9). Note that the solution provides only approximations

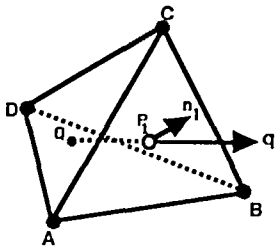

Figure 8 Upwind differencing on a tetrahedral mesh

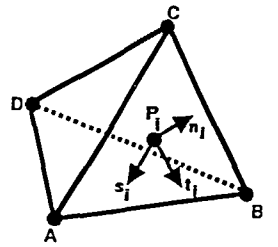

Figure 9 A local coordinate system

to the normal component of the velocity vector $\mathbf{q}$ at the circumcentres of tetrahedral faces. In the next section we discuss the recovery of approximations to the velocity *vector* at these same N_F points in the flow region.

RECONSTRUCTION OF VELOCITY FIELD

Inherent in the covolume method is the need to reconstruct the (vector) velocity field $\mathbf{q}$ given components of $\mathbf{q}$ at various points in the flow region[5,6,13,14,17–19]. In References 19 and 13, schemes were presented for triangular meshes (2D problems) that reproduce *constant* flow fields exactly. These may not be of sufficient accuracy for use in discretizations like the upwind scheme presented earlier. A reconstruction procedure for triangulations was presented[15] that reproduces *linear* flow fields exactly. We now extend this procedure to three-dimensional tetrahedral meshes.

We introduce a local coordinate system on each of the tetrahedral faces. The system is centered at the circumcentre P_i of the ith face and $\mathbf{n}_i$ is the pre-assigned unit normal to the ith face. The remaining coordinate directions $\mathbf{s}_i$ and $\mathbf{t}_i$ are chosen in the plane of the ith face so that $\mathbf{s}_i$, $\mathbf{t}_i$ and $\mathbf{n}_i$ form a (non-orthogonal) right handed system. For example, a convenient choice for $\mathbf{s}_i$ and $\mathbf{t}_i$ are unit vectors in the directions $\overline{\mathbf{AC}}$ and $\overline{\mathbf{CB}}$ in *Figure 9*.

Given a tetrahedron Ω_1, let Ω_j, $j = 2, 3, 4, 5$ be the four tetrahedra sharing a face with Ω_1 (see *Figure 10*). Let $\{P_i\}_{i=1}^{16}$ be the 16 facial circumcentres of these four neighbouring tetrahedra. At P_j the velocity $\mathbf{q}$ is approximated by:

$$\mathbf{q}_j(t) = u_j(t)\mathbf{n}_j + v_j(t)\mathbf{s}_j + w_j(t)\mathbf{t}_j \tag{24}$$

where u_j is known and we seek values for v_j and w_j, $j = 1, \ldots, 16$. These 32 components are chosen so as to reproduce an arbitrary *linear* flow field (in $\cup_{j=1}^{5} \Omega_j$) of the form:

$$\mathbf{q}(t) = \mathbf{a}_0(t) + \mathbf{a}_1(t)x + \mathbf{a}_2(t)y + \mathbf{a}_3(t)z \tag{25}$$

where the four 3-vectors $\mathbf{a}_i(t)$ are fixed but arbitrary. Thus, there are a total of 44 unknowns. Equating (24) and (25) at each of the 16 circumcentres yields 48 scalar equations in 44 unknowns. We have yet to investigate the rank of this system, but our experience in the two-dimensional case suggests it is of full rank. As such a least squares procedure can be used for its solution. Also, as in 2D, we anticipate that the solution of this system can be obtained by solving a much smaller reduced least squares problem. (See Reference 15 for details of this procedure in the 2D case.)

DUAL VARIABLE METHOD

We present a variable reduction technique which replaces the $N_F + N_T$ system (11), (23) by an equivalent system of dimension $N_F - N_T$. This network method (the *dual variable method*) was presented[1,11,12,21,22] for rectangular grids and[5,6,13–15,23] for triangular grids.

In network terminology[2] the edges (links) and vertices (nodes) of the Voronoi polytopes form a directed network Γ, while those of the Delaunay tessellation constitute its dual Γ^*. Each link

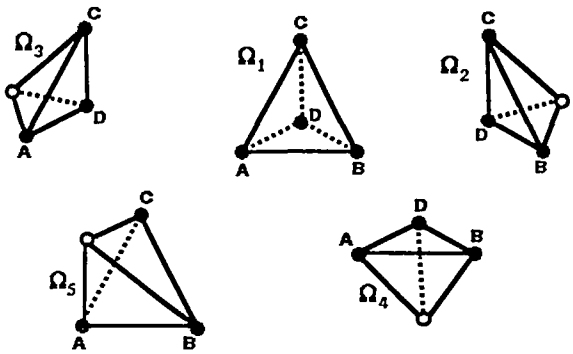

Figure 10 A tetrahedron Ω_1 and its four neighbouring tetrahedra

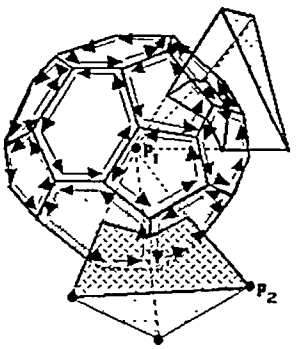

Figure 11 Elementary cycles

of Γ carries a *flow* that is an approximation of the velocity component normal to a face of a tetrahedron, and each node of Γ carries a *state* that is an approximation of the pressure at the circumcentre of a tetrahedron. The matrix A in (11) is the *incidence matrix* of the network Γ, equations (11) are its node laws and equations (23) constitute the *link characteristics*.

The dual variables are states on the nodes of Γ^*, i.e. the vertices of the tetrahedra. If the flow region is simply connected, then the boundaries of the faces of the Voronoi polytopes are *elementary cycles* in Γ. An elementary cycle is a closed path of links in the network such that in a complete traverse of the cycle a node is encountered exactly once. In two dimensions an edge of a Voronoi polygon is shared by at most two polygons, and the boundaries of the Voronoi polygons form a basis of elementary cycles. However, in three dimensions, an edge of a Voronoi polytope may be common to 3 or more polytopes. Hence, the set of all elementary cycles that are boundaries of faces of polytopes yield a dependent set. For example, in *Figure 11*, the elementary cycles corresponding to facial boundaries for a simple Voronoi polytope are indicated. Note that the elementary cycle on face $\mathbf{F}_{p_1p_2}$ is just the negative of the sum of the other elementary cycles associated with faces of this polytope.

The dimension of the ker A or the number of elementary cycles in a basis for ker A is $N_F - N_T$. The ker A is the kernel or null space of A: the set of linearly independent vectors $\{\mathbf{C}_1, \mathbf{C}_2, \ldots, \mathbf{C}_{N_F-N_T}\}$ which satisfy $\mathbf{AC}_i = 0$. In theory, (Reference 2, Theorem 7, p. 131) it is straightforward to construct an $N_F \times (N_F - N_T)$ fundamental matrix C whose columns $\{\mathbf{C}_i\}_{i=1}^{N_F-N_T}$ are cycle vectors for elementary cycles of Γ and form a basis for ker A.

Given the fundamental matrix C such that $\mathbf{AC} = 0$ we proceed to reduce the size of the primitive system as follows. If we let $\mathbf{D}_1\mathbf{u}_0$ be any particular solution of the discrete continuity equation (11), then $(\mathbf{D}_1\mathbf{u} - \mathbf{D}_1\mathbf{u}_0) \in \ker \mathbf{A}$. Such a particular solution can be obtained using the notion of a spanning tree[2] for Γ, Reference 2. Hence $\mathbf{D}_1\mathbf{u} - \mathbf{D}_1\mathbf{u}_0 = \mathbf{C}\gamma$ for some vector of *dual variables* $\gamma = (\gamma_1, \gamma_2, \ldots, \gamma_{N_F-N_T})^T$, and

$$\mathbf{u} = \mathbf{D}_1^{-1}(\mathbf{C}\gamma + \mathbf{D}_1\mathbf{u}_0) \tag{26}$$

Equation (26) expresses the N_F unknown normal components of velocity in terms of the $(N_F - N_T)$ dual variables. If we substitute (26) into (23), we have a system of N_F ordinary differential equations in the $(N_F - N_T)$ components of γ and the N_T components of $\mathbf{p}$. However, it is also possible to eliminate the pressures from this equation since $\mathbf{C}^T\mathbf{A}^T = (\mathbf{AC})^T = 0$. Multiply (23) by $\mathbf{C}^T\mathbf{D}_2$, after substituting (26) into (23), to obtain:

$$(\mathbf{C}^T\mathbf{D}_2\mathbf{D}_1^{-1}\mathbf{C})\frac{d\gamma}{dt} + \mathbf{C}^T\mathbf{D}_2Q(\gamma)\mathbf{D}_1^{-1}\mathbf{C}\gamma = \mathbf{C}^T\mathbf{D}_2(\mathbf{b} - Q(\gamma)\mathbf{u}_0) \tag{27}$$

This is a system of $N_F - N_T$ ordinary differential equations for γ.

Ignoring the faces of tetrahedra in common to $\partial\Omega$ where pressures may be specified, it is known[7] that N_T (the number of tetrahedra) is approximately $\frac{1}{2}N_F$ (the number of internal faces). Hence the primitive system is of dimension $N_F + N_T \doteq 3N_T$ and the dual variable system is of dimension $N_F - N_T \doteq N_T$, for a *reduction factor* of 3.

RELATIONSHIP TO THE MAC METHOD

The MAC scheme[15] is a much used finite difference technique for approximating the incompressible Navier–Stokes equations. Although it can only be used with hexahedral meshes, it does offer great simplicity and the programming convenience of a rectangular geometry. In order to provide some credibility for the covolume method described herein, we show how for an appropriately chosen tetrahedral mesh the MAC scheme can be reproduced by this method for the simple steady-state Stokes equations.

We briefly review the MAC approach for the case of a uniform hexahedral mesh of gauge h. The variables used (velocity components normal to and passing through the centre of cell faces, pressures at cell circumcentres) are illustrated in *Figure 12*.

The MAC approximation to the continuity equation is given by:

$$\frac{u_{i,j,k} - u_{i-1,j,k}}{h} + \frac{v_{i,j,k} - v_{i,j-1,k}}{h} + \frac{w_{i,j,k} - w_{i,j,k-1}}{h} = 0 \tag{28}$$

The x-momentum equation for the Stokes model at P is (for unit viscosity):

$$\begin{aligned} &-\frac{u_{i+1,j,k} - 2u_{i,j,k} + u_{i-1,j,k}}{h^2} \\ &-\frac{u_{i,j+1,k} - 2u_{i,j,k} + u_{i,j-1,k}}{h^2} \\ &-\frac{u_{i,j,k+1} - 2u_{i,j,k} + u_{i,j,k-1}}{h^2} \\ &+\frac{p_{i,j,k} - p_{i-1,j,k}}{h} = F_{x;i,j} \end{aligned} \tag{29}$$

The only modification to these equations occurs at flow boundaries.

A tetrahedral complementary volume scheme which produces equations equivalent to (28),

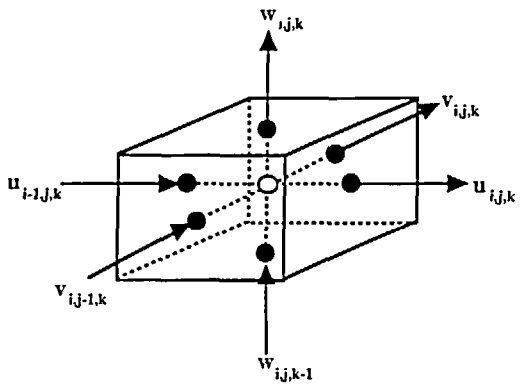

Figure 12 The MAC placement of variables

(29) can be obtained as follows. Consider the decomposition of the curve in *Figure 12* into 5 abutting tetrahedra as illustrated in *Figure 13*. The tetrahedra labelled I, II, III, and IV are identical right tetrahedra each bounded by three faces that are isosceles right triangles and one face that is an equilateral triangle. The 5th tetrahedra, labelled V in *Figure 13*, has a boundary composed of four identical equilateral triangles each of area $A = 3h^2/2\sqrt{3}$. All five tetrahedra share the same circumcentre, namely the circumcentre of the cube in *Figure 12*. The circumcentres of any right triangular face of a tetrahedron falls at the centre of the associated hypotenuse; the circumcentres of equilateral triangular faces lie at associated triangle centroids. Note that, in general, there is one normal velocity component for each triangular face in the tetrahedral mesh. However, right triangles that abutt along a common hypotenuse (like **CAB** and **CBD** in *Figure 13*) share identical circumcentres (the point *P*), therefore identical normals. Hence the linear steady state form of (9) is implemented twice at *P* (once for face **CAB** and once for face **CBD**) and the resulting difference equations are added to produce a single difference equation associated with the point *P*.

In the covolume scheme described in an earlier section, the pressure variables are defined at the five tetrahedral circumcentres which coincide with the centroid of the cube in *Figure 12*. We treat these five pressure variables as being the same and at a location that coincides with the MAC placement of pressure. Consider tetrahedron *V* and let $\mathbf{n}_1$, $\mathbf{n}_2$, $\mathbf{n}_3$, and $\mathbf{n}_4$ be inward pointing normals passing through the circumcentres of faces **CFH**, **CBH**, **CBF**, and **BFH** respectively in *Figure 13*. The remaining normals involved are assumed to be in the positive coordinate direction (see *Figure 13*). To obtain (28), we integrate the continuity equation over each of the five tetrahedra in *Figure 13* as outlined earlier (see (10)). The resulting five flux equations are, then:

$$\int\int_{\partial I} \mathbf{q}\cdot\mathbf{n}\,d\sigma \simeq \frac{h^2}{2}(-u_{i-1,j,k} - v_{i,j-1,k} - w_{i,j,k-1}) + A(\mathbf{q}\cdot\mathbf{n}_1) = 0$$

$$\int\int_{\partial II} \mathbf{q}\cdot\mathbf{n}\,d\sigma \simeq \frac{h^2}{2}(u_{i,j,k} - v_{i,j-1,k} + w_{i,j,k}) + A(\mathbf{q}\cdot\mathbf{n}_2) = 0$$

$$\int\int_{\partial III} \mathbf{q}\cdot\mathbf{n}\,d\sigma \simeq \frac{h^2}{2}(u_{i,j,k} - w_{i,j,k-1} + v_{i,j,k}) + A(\mathbf{q}\cdot\mathbf{n}_3) = 0$$

$$\int\int_{\partial IV} \mathbf{q}\cdot\mathbf{n}\,d\sigma \simeq \frac{h^2}{2}(-u_{i-1,j,k} + v_{i,j,k} + w_{i,j,k}) + A(\mathbf{q}\cdot\mathbf{n}_4) = 0$$

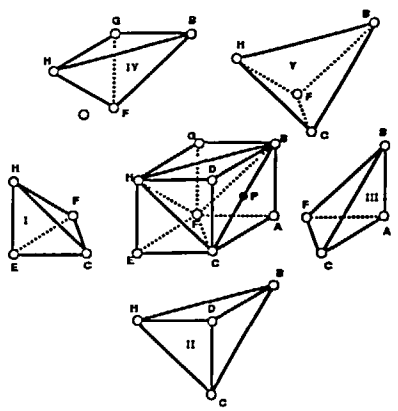

Figure 13 Tetrahedral decomposition of cube

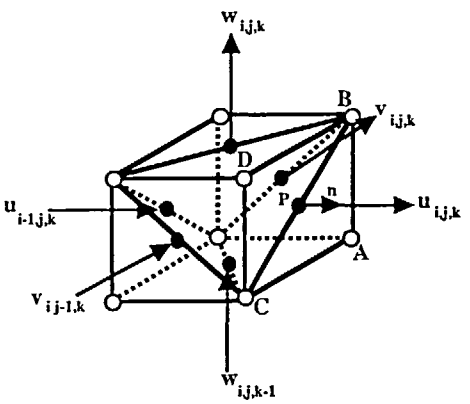

Figure 14 Assignment of velocity components

$$\int\int_{\partial V} \mathbf{q}\cdot\mathbf{n}\, d\sigma \simeq -A\mathbf{q}\cdot(\mathbf{n}_1 + \mathbf{n}_2 + \mathbf{n}_3 + \mathbf{n}_4)$$

Adding these gives:

$$h^2(u_{i,j,k} - u_{i-1,j,k} + v_{i,j,k} - v_{i,j-1,k} + w_{i,j,k} - w_{i,j,k-1}) = 0 \tag{30}$$

which is equivalent to (28), the discrete continuity equation for the MAC scheme.

Now, let $\mathbf{n}$ denote the outward pointing normal to face **ABCD** that passes through the circumcentre bisecting the edge **BC** (see *Figure 14*).

The Voronoi polytope associated with node **A** (itself a cube of dimension h) has a boundary consisting of the hyperplanes that bisect the six edges in the mesh that contain node **A**. Two of those planes P_1, P_2 are shown in *Figure 15* together with flow and pressure labels attached to the edges of the polyhedron. In *Figure 16* we show two hyperplanes, P_3, P_4 on the surface of the Voronoi polytope containing node **D**. *Figures 15* and *16* indicate that the hyperplane in the Voronoi diagram that bisects the edge **BC** is the line defined by the intersections of P_1, P_2, P_3, P_4; that is, the line connecting circumcentres $p_{i-1,j,k}$ and $p_{i,j,k}$. This degeneracy would imply that area $(\mathbf{F}_{\mathbf{BC}}) = 0$ in (17), hence (17) cannot be used to define a difference equation in this case. Rather, we do not discretize $(\mathbf{curl}\,\mathbf{q})_{(\mathbf{B}+\mathbf{C})/2}\cdot\mathbf{T}_{\mathbf{BC}}$ in (16) via (17)–(20), but rely on the cancellation of this term from the difference system by adding the difference equations that arise when $\mathbf{n}_1$ in (14) is chosen on face **CAB** and when $\mathbf{n}_1$ is chosen on face **CBD** in *Figure 13*. Applying (14)–(16) to this regular mesh gives:

$$\mathbf{curl}(\mathbf{curl}\,\mathbf{q})\cdot\mathbf{n} \simeq \frac{2}{h^2}\left(h\,\mathbf{curl}\,\mathbf{q}\cdot\mathbf{T}|_{(\mathbf{A}+\mathbf{B})/2} + h\,\mathbf{curl}\,\mathbf{q}\cdot\mathbf{T}|_{(\mathbf{A}+\mathbf{C})/2} + \sqrt{2}\,h\,\mathbf{curl}\,\mathbf{q}\cdot\mathbf{T}|_{(\mathbf{B}+\mathbf{C})/2}\right) \tag{31}$$

From the analogues of (17)–(19) we have:

$$\mathbf{curl}\,\mathbf{q}\cdot\mathbf{T}|_{(\mathbf{C}+\mathbf{A})/2} \simeq \frac{1}{h^2}(hu_{i,j,k} - hw_{i,j,k} - hu_{i,j,k-1} + hw_{i-1,j,k}) \tag{32}$$

$$\mathbf{curl}\,\mathbf{q}\cdot\mathbf{T}|_{(\mathbf{A}+\mathbf{B})/2} \simeq \frac{1}{h^2}(hu_{i,j,k} + hv_{i,j+1,k} - hu_{i,j+1,k} - hv_{i-1,j-1,k}) \tag{33}$$

Therefore, the steady-state form of (9) without the convection term (that is, the scalar Stokes

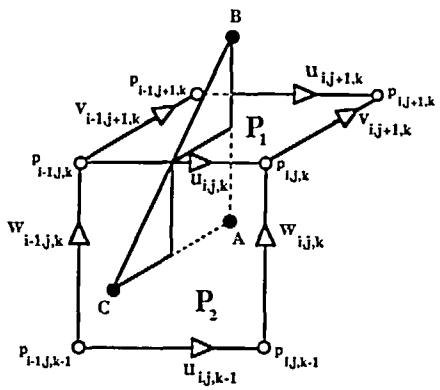

Figure 15 Two square faces of polytope associated with **B**

Figure 16 Two square faces of polytope associated with **D**

model) can be approximated using (31)–(33) as:

$$\frac{2}{h^2}(-u_{i,j,k-1} + 2u_{i,j,k} - u_{i,j+1,k} + v_{i,j+1,k} - v_{i-1,j+1,k} + w_{i-1,j,k} - w_{i,j,k} + \sqrt{2}\,h\,\mathbf{curl}\,\mathbf{q}\cdot\mathbf{T}|_{(B+C)/2}) + \frac{p_{i,j,k} - p_{i-1,j,k}}{h} = \mathbf{F}_{x;i,j,k} \quad (34)$$

With reference to *Figure 16*, a similar implementation of (14)–(16) arising from tetrahedron **CBDH** in *Figure 13* produces:

$$\frac{2}{h^2}(-u_{i,j-1,k} + 2u_{i,j,k} - u_{i,j,k+1} + w_{i,j,k+1} - w_{i-1,j,k+1} + v_{i-1,jk} - v_{i,j,k} - \sqrt{2}\,h\,\mathbf{curl}\,\mathbf{q}\cdot\mathbf{T}|_{(B+C)/2}) + \frac{p_{i,j,k} - p_{i-1,j,k}}{h} = \mathbf{F}_{x;i,j,k} \quad (35)$$

From the continuity equation:

$$u_{i+1,j,k} - u_{i,j,k} + v_{i,j+1,k} - v_{i,j,k} + w_{i,j,k+1} - w_{i,j,k} = 0 \quad (36)$$

$$u_{i,j,k} - u_{i-1,j,k} + v_{i-1,j+1,k} - v_{i-1,j,k} + w_{i-1,j,k,+1} - w_{i-1,j,k} = 0 \quad (37)$$

Adding the two scalar momentum equations (34) and (35), and multiplying by $\frac{1}{2}$ gives:

$$-\frac{u_{i,j+1,k} - 2u_{i,j,k} + u_{i,j-1,k}}{h^2} - \frac{u_{i,j,k+1} - 2u_{i,j,k} + u_{i,j,k-1}}{h^2} + Q + \frac{p_{i,j,k} - p_{i-1,j,k}}{h} = \mathbf{F}_{x;i,j,k} \quad (38)$$

where Q is given by:

$$h^2 Q = -v_{i-1,j+1,k} + v_{i,j+1,k} - v_{i,j,k} + v_{i-1,j,k} - w_{i,j,k} + w_{i-1,j,k} - w_{i-1,j,k+1} + w_{i,j,k+1} \quad (39)$$

Subtracting (37) from (36) shows that:

$$Q = -\frac{u_{i+1,j,k} - 2u_{i,j,k} + u_{i-1,j,k}}{h^2} \quad (40)$$

and (38) is the same as (29), the x-momentum equation for the MAC scheme.

These calculations show the equivalence of the two methods in the uniform hexahedral mesh case and demonstrate that the covolume scheme presented here provides a generalization of the MAC scheme to general three-dimensional tessellations composed of tetrahedra.

CONCLUSIONS

Earlier[5,6,13–15] we presented an approach that integrates three computatioual components into a single algorithm for modelling the two-dimensional incompressible Navier–Stokes equations: (1) automatic Delaunay mesh generation, (2) covolume finite difference equation generation, and (3) dual variable reduction of primitive systems. This covolume approach replaces the continuum problem involving a vector velocity field with a discrete problem involving only a

single scalar velocity which is normal to triangle sides. Also presented[15] was an interpolation scheme for deriving *a posteriori* approximations of flows tangent to triangle sides in order to produce a discrete vector-valued approximation of velocity. This two-dimensional implementation has been quite successful.

In this paper we have extended this approach to the modelling of the three-dimensional incompressible Navier–Stokes equations. The primitive discrete model results from the approximation of velocity components tangent to boundary edges on Voronoi polyhedral covolumes (normal to tetrahedral faces) and the pressure field approximated at the corners of the polyhedral surface (the circumcentres of Delaunay tetrahedra). We have given details on the implementation of this model for *ideal* tessellations as well as for the more realistic tessellations that arise when using current solid mesh generation software. While we have not completely answered all questions for tessellations of the latter type, we do not forsee any insurmountable problems with the three-dimensional implementation. We have also shown how the MAC scheme can be derived as a special case of the covolume scheme presented here.

As in two dimensions, the DAEs generated by the covolume method in three dimensions are well suited for variable reduction by the dual variable method. The primitive DAE system can be replaced by an equivalent system of ODEs whose dimension is a factor of *three* smaller than that of the primitive system.

REFERENCES

1 Amit, R., Hall, C. A. and Porsching, T. A. An application of network theory to the solution of implicit Navier–Stokes difference equations, *J. Comp. Phys.*, **40**, 183–201 (1981)
2 Berge, C. and Ghouila-Houri, A. *Programming, Games and Transportation Networks*, Methuen, London (1965)
3 Cavendish, J. C., Field, D. A. and Frey, W. H. An approach to automatic three-dimensional finite element mesh generation, *Int. J. Num. Meth. Eng.*, **21**, 329–347 (1985)
4 Cavendish, J. C., Field, D. A. and Frey, W. H. Automatic mesh generation: a finite element/computer aided design interface, *The Mathematics of Finite Elements and Applications V*, Academic Press, San Diego (1985)
5 Cavendish, J. C., Hall, C. A. and Porsching, T. A. Solution of incompressible Navier–Stokes equations on unstructured grids using dual tessellations, *Int. J. Num. Meth. Heat Fluid Flow*, **2**, 483–502 (1992)
6 Cavendish, J. C. and Hall, C. A. A complementary volume approach for modelling incompressible Navier–Stokes equations on Delaunay/Voronoi tessellations, *Proc. 7th Int. Conf. Num. Meth. Lamin. Turbul. Flows*, Stanford Univ. (1991)
7 Ewing, D. J., Fawkes, A. J. and Griffiths, J. R. Rules governing the number of nodes and elements in a finite element mesh, *Int. J. Num. Meth. Eng.*, **2**, 597–601 (1970)
8 Finney, J. L. A procedure for the construction of Voronoi polyhedra, *J. Comp. Phys.*, 137–143 (1979)
9 Frey, W. H. and Cavendish, J. C. Fast planar mesh generation using the Delaunay triangulation, *General Motors Research Publication GMR-4555* (1983)
10 Frey, W. H. Selective refinement: a new strategy for automatic node placement in graded triangular meshes, *Int. J. Num. Meth. Eng.*, **24**, 2183–2200 (1987)
11 Gustafson, K. and Hartman, R. Graph theory and fluid dynamics, *SIAM J. Algeb. Disc. Meth.*, **8**, 643–656 (1985)
12 Hall, C. A. Numerical solution of Navier–Stokes problems by the dual variable method, *SIAM J. Alg. Disc. Meth.*, **6** (1985), 220–236.
13 Hall, C. A., Cavendish, J. C. and Frey, W. H. The dual variable method for solving fluid flow difference equations on Delaunay triangulations, *Comp. Fluids*, **20**, 145–164 (1991)
14 Hall, C. A., Porsching, T. A. and Mesina, G. L. On a network method for unsteady incompressible fluid flow on triangular grids, *Int. J. Num. Meth. Fluids*, **15**, 1383–1406 (1992)
15 Hall, C. A., Porsching, T. A. and Hu, P. Covolume-dual variable method for thermally expandable flow on unstructured triangular grids, *Comp. Fluid Dyn.*, **2**, 111–139 (1994)
16 Harlow, F. H. and Welch, F. E. Numerical calculations of time dependent viscous incompressible flow of fluid with a free surface, *Phys. Fluids*, **8**, 2182 (1965)
17 Nicolaides, R. A. Flow discretization by complementary volume techniques, *Proc. 9th AIAA CFD Meet.*, Buffalo, N.Y. AIAA Paper 89-1978 (1989)
18 Nicolaides, R. A. Triangular discretization for the vorticity–velocity equations, *Proc. 7th Int. Conf. Finite Elements in Flow Problems, Huntsville*, p. 1 (1989)
19 Nicolaides, R. A. Direct discretization of planar *div-curl* problems, *SIAM J. Num. Anal.*, **29**, 32 (1992)
20 Peyret, R. and Taylor, T. D. *Computational Methods for Fluid Flow*, Springer, Berlin (1983)
21 Porsching, T. A. A network model for two-fluid, two phase flow, *Num. Meth. Part. Diff. Eqs.*, **1**, 295–313 (1985)

22 Porsching, T. A. A finite difference method for thermally expandable fluid transients, *Nucl. Sci. Engng.*, **64**, 177 (1977)
23 Porsching, T. A. and Hall, C. A. A network method for homogeneous, thermally expandable two-phase flow on unstructured triangular grids, *Proc. Fifth Int. Top. Meet. Nucl. React. Therm. Hydraulics, Salt Lake City*, pp. 1767–1774 (1992)
24 Sibson, R. Locally equiangular triangulations, *Computer J.*, **21**, 243–245 (1978)
25 Watson, D. F. Computing the *n*-dimensional Delaunay tessellation with applications to Voronoi polytopes, *Computer J.*, **24**, 167 (1981)
26 Wu, X. Analysis and applications of the covolume method for the Navier–Stokes equations, *PhD Dissert.*, Carnegie Mellon University (1991)